OXFORD

SOT | Society of Toxicology
www.toxsci.oxfordjournals.org

TOXICOLOGICAL SCIENCES, 170(1), 2019, 57–68

doi: 10.1093/toxsci/kfz077
Advance Access Publication Date: March 23, 2019
Research Article

Delayed Treatment With 4-Methylpyrazole Protects Against Acetaminophen Hepatotoxicity in Mice by Inhibition of c-Jun n-Terminal Kinase

Jephte Y. Akakpo,* Anup Ramachandran,* Luqi Duan,* Matthew A. Schaich,† Matthew W. Jaeschke,* Bret D. Freudenthal,† Wen-Xing Ding,* Barry H. Rumack,‡ and Hartmut Jaeschke*,[1]

*Department of Pharmacology Toxicology & Therapeutics and †Department of Biochemistry and Molecular Biology, University of Kansas Medical Center, Kansas City, Kansas 66160; and ‡Department of Emergency Medicine and Pediatrics, University of Colorado School of Medicine, Aurora, Colorado 80045

[1]To whom correspondence should be addressed at Department of Pharmacology, Toxicology & Therapeutics, University of Kansas Medical Center, 3901 Rainbow Blvd, MS 1018, Kansas City, KS 66160. Fax 913 588 7501; E-mail: hjaeschke@kumc.edu.

ABSTRACT

Acetaminophen (APAP) overdose is the most common cause of hepatotoxicity and acute liver failure in the United States and many western countries. However, the only clinically approved antidote, N-acetylcysteine, has a limited therapeutic window. 4-Methylpyrazole (4MP) is an antidote for methanol and ethylene glycol poisoning, and we have recently shown that cotreatment of 4MP with APAP effectively prevents toxicity by inhibiting Cyp2E1. To evaluate if 4MP can be used therapeutically, C57BL/6J mice were treated with 300 mg/kg APAP followed by 50 mg/kg 4MP 90 min later (after the metabolism phase). In these experiments, 4MP significantly attenuated liver injury at 3, 6, and 24 h after APAP as shown by 80%–90% reduction in plasma alanine aminotransferase activities and reduced areas of necrosis. 4MP prevented c-Jun c-Jun N-terminal kinase (JNK) activation and its mitochondrial translocation, and reduced mitochondrial oxidant stress and nuclear DNA fragmentation. 4MP also prevented JNK activation in other liver injury models. Molecular docking experiments showed that 4MP can bind to the ATP binding site of JNK. These data suggest that treatment with 4MP after the metabolism phase effectively prevents APAP-induced liver injury in the clinically relevant mouse model *in vivo* mainly through the inhibition of JNK activation. 4MP, a drug approved for human use, is as effective as N-acetylcysteine or can be even more effective in cases of severe overdoses with prolonged metabolism (600 mg/kg). 4MP acts on alternative therapeutic targets and thus may be a novel approach to treatment of APAP overdose in patients that complements N-acetylcysteine.

Key words: acetaminophen hepatotoxicity; c-Jun N-terminal kinase; autophagy; mitochondria; N-acetylcysteine; galactosamine-endotoxin.

Acetaminophen (APAP) is one of the most widely used analgesic and antipyretic drugs worldwide. Although considered safe at therapeutic levels, intentional or unintentional overdoses can cause extensive hepatotoxicity and even acute liver failure in both animals and humans (Yoon *et al.*, 2016). Early mechanistic studies identified the formation of a reactive metabolite, presumably N-acetyl-*p*-benzoquinone imine (NAPQI), glutathione (GSH) depletion and protein adduct formation as critical events in the pathophysiology (Mitchell *et al.*, 1973; Nelson, 1990). This insight into the mechanism of toxicity led to the rapid introduction of N-acetylcysteine (NAC) as a clinical antidote against APAP overdoses in the 1970s (Rumack and Bateman, 2012). Since that time, the mechanistic understanding of APAP-induced cell death and liver injury increased dramatically (Jaeschke *et al.*, 2012; Ramachandran and Jaeschke, 2018); however, this increased knowledge did not translate into additional

drugs for clinical use. There are 2 main reasons for the lack of new drugs for this indication. First, NAC is highly effective in preventing and limiting liver injury in patients, especially when given early (within 10 h) after the overdose. NAC supports the rapid resynthesis of GSH, which can assist in detoxifying NAPQI (Corcoran and Wong, 1986), but also scavenges peroxynitrite and reactive oxygen species (ROS) and the metabolites of NAC can support mitochondrial bioenergetics (Saito *et al.*, 2010b). These diverse mechanisms allow NAC to be effective over a significant time frame (Smilkstein *et al.*, 1988). The second reason for the lack of new drugs on the market is the high costs of *de novo* drug development. Although more than 70 000 patients are hospitalized each year because of an APAP overdose and around 50% of all cases of acute liver failure in the United States are due to APAP hepatotoxicity (Budnitz *et al.* 2011; Manthripragada *et al.* 2011), this patient population is still too limited to justify these costs. Therefore, a more realistic possibility for new therapeutics is the repurposing of existing drugs that have already been shown to be safe in humans.

4-Methylpyrazole (4MP, fomepizole) is a competitive inhibitor of alcohol dehydrogenase. It is clinically used as an antidote against methanol and ethylene glycol poisoning (Barceloux *et al.*, 1999; Bekka *et al.*, 2001; Bestic *et al.*, 2009; Brent *et al.*, 2001). In a recent case report of a patient who took a large overdose of APAP with ethanol, the patient was successfully treated with both 4MP and with NAC (Zell-Kanter *et al.*, 2013). It was subsequently hypothesized that the beneficial outcome in this case may have been affected by the cotreatment with 4MP (Yip and Heard, 2016). Based on these clinical observations and *in vitro* studies that showed inhibition of cytochrome P450 (CYP)2E1 by 4MP in human microsomes (Dai and Cederbaum, 1995; Hazai *et al.*, 2002), we investigated the potential efficacy of 4MP in a murine APAP hepatotoxicity model and in human hepatocytes (Akakpo *et al.*, 2018). Using a cotreatment regimen, we demonstrated that 4MP eliminated APAP-induced liver injury by inhibiting P450 enzymes and therefore prevented oxidative metabolism with reactive metabolite formation, GSH depletion and the generation of protein adducts (Akakpo *et al.*, 2018). However, inhibition of P450 enzymes alone would be of limited benefit as many patients seek medical attention well into the metabolism phase and the progression of liver injury. Therefore, the objective of the current study was to assess if a delayed treatment with 4MP, ie, after the metabolism of APAP is completed, is still protective and to investigate the potential mechanism.

MATERIALS AND METHODS

Animals and experimental design. Experiments requiring animal procedures were approved by the Institutional Animal Care and Use Committee of the University of Kansas Medical Center (KUMC). In this study, 8 to 12 weeks old C57BL/6J male mice (Jackson Labs, Bar Harbor, Maine) were utilized. Animals were adapted to the KUMC animal facility with unrestricted access to food and water for at least 5 days. Then, animal procedures were performed following the National Research Council for the care and use of laboratory animals' guidelines.

After a 15 h overnight fast, animals were subjected to ip injections of either 300 or 600 mg/kg APAP (Sigma-Aldrich, St Louis, Missouri). Ninety minutes post-APAP, mice received a single treatment of 50 or 200 mg/kg 4MP (Brennan *et al.*, 1994; Kucukardali *et al.*, 2002) (Sigma-Aldrich), 500 mg/kg NAC (Sigma-Aldrich), or a combined treatment of 4MP+NAC. Mice were euthanized under isoflurane anesthesia at 3, 6, and 24 h time points post-APAP followed by collection of blood and liver samples.

Biochemical assays. The level of APAP-induced hepatic injury was assessed by measuring plasma alanine aminotransferase (ALT) activity with a kit purchased from Pointe Scientific (Canton, Michigan). Total liver hepatic GSH and glutathione disulfide (GSSG) was measured using a modified Tietze assay as described in detail (McGill and Jaeschke, 2015).

Histology. To assess the extent of liver damage, 10% formalin fixed liver tissue samples were embedded in paraffin and cut into 5 μm sections for evaluation of necrotic cell death and nuclear DNA fragmentation. Hepatic necrosis was assessed with hematoxylin and eosin (H&E) staining and DNA fragmentation was assessed using the terminal deoxynucleotidyl transferase dUTP nick end labeling (TUNEL) with the *in-situ* Cell Death Detection assay (Roche, Indianapolis, New Jersey) as described (Gujral *et al.*, 2002).

Antibodies and reagents. All primary antibodies (1:1000 dilution) used in this study were purchased from Cell Signaling Technology located in Danvers, Massachusetts. Western blot experiments were performed as described (Akakpo *et al.*, 2018) with rabbit anti-JNK (c-Jun N-terminal kinase) antibody (Cat. No. 9252), rabbit antiphospho-JNK antibody (Cat. No. 4668), rabbit anti-AIF (apoptosis-inducing factor) antibody (Cat. No. 5318), rabbit LC3 antibody (Cat. No. 2775), and rabbit ß-actin antibody (Cat. No. 4967). To detect protein bands of interest, antirabbit IgG horseradish peroxidase coupled secondary antibody (1:5000 dilution) was purchased from Santa Cruz. Bands were detected via chemiluminescence with the Licor Odyssey imaging system (LICOR Biosciences).

APAP protein adducts. Liver homogenates were filtered through a Bio-Spin 6 column (Bio-Rad, Hercules, California) to remove low molecular weight metabolites that could interfere with detection of APAP protein adducts (McGill *et al.*, 2012b). The filtrate, which included proteins with APAP bound to cysteine residues, was digested for 15 h at 50°C in a 1:1 ratio with 8 U/ml Streptomyces griseus solution. This digestion liberated the APAP-Cys adducts from the cellular proteins. The protein derived APAP-Cys residues were filtered and detected via HPLC with an electrochemical detector (Coularray, ESA Biosciences, Chelmsford, Massachusetts).

Molecular docking. AutoDock Vina was used to perform all molecular docking experiments (Trott and Olson, 2010). The models used for docking include JNK1, JNK2, and Cyp2e1 (PDB codes 3V3V, 3NPC, and 3E4E, respectively) (Baek *et al.*, 2013; Kuglstatter *et al.*, 2010; Porubsky *et al.*, 2008). Each of these structures was published bound to a ligand, so each structure was prepared for molecular docking by removing their ligands and any solvent molecules. Auto-DockTools 4.2 was used to add polar hydrogens, Gasteiger charges, and to position a grid box large enough to encompass each protein in whole (in each case, this was a 60 × 60 × 60 Å cube) (Morris *et al.*, 2009). To account for the search box larger than 27 000 Å, search exhaustiveness was raised to 100. Coordinates of the compounds of interest were taken from previously published structures (PDB codes 3V3V, 3NPC, and 3E4E), and then prepared for molecular docking using Auto-DockTools 4.2, allowing full ligand flexibility (Adams *et al.*, 2010). In each case, a control molecular docking experiment was performed with the published ligand, to ensure the

appropriateness of AutoDock Vina to analyze the binding sites of these proteins, and in each case the RMSD of the control docking was less than 2 Å.

Cellular thermal shift assay. A liver sample was collected from untreated C57BL/6J mice and placed into a 1.5 ml Eppendorf tube. The sample was then frozen using liquid nitrogen and homogenized in RIPA buffer (10 mM Tris-Cl [pH 8.0], 1 mM EDTA, 1% Triton X-100, 0.1% sodium deoxycholate, 0.1% SDS, 140 mM NaCl, 1 mM PMSF), supplemented with protease inhibitors. The resulting homogenate was centrifuged at 4°C for 10 min at 14 000 × g. Then, 100 µl of the supernatant was transferred into 7 individual 1.5 ml Eppendorf tubes and 10 µl of a 20 mM 4MP stock solution was added. After a 30-min incubation at 37°C, 1 tube was kept at room temperature whereas the remaining 6 tubes were subjected to transient heating at 50°C, 52°C, 54°C, 56°C, 58°C, and 60°C for 8 min. Subsequently, a controlled cooling step at room temperature for 3 min was performed. All 7 samples were then freeze thawed in liquid nitrogen 3 times and spun at 4°C for 20 min at 20 000 × g to remove precipitated protein. Finally, the remaining soluble protein in the supernatant was subjected to electrophoresis and western blotting for JNK and quantified by densitometry (Ishii *et al.*, 2017; Mateus *et al.*, 2016).

In vitro c-Jun n-terminal kinase assay. JNK activity was assayed *in vitro* using a c-Jun recombinant protein as the substrate. Phospho-JNK was immunoprecipitated from liver homogenates (500 µg protein) of animals treated with D-galactosamine-endotoxin (Gal-ET) for 1 h, using an anti-P-JNK antibody (Cell Signaling Technology, No. 9255) bound to Dynabead protein G (ThermoFisher Scientific). The beads were washed, followed by incubation with 1µg GST-c-Jun (1–79) fusion protein (BioVision, Inc, Mountain View, California) either with or without 2 mM 4MP in kinase buffer (10 mM $MgCl_2$, 50 mM Tris-HCl, 1 mM EGTA, and 50 µM ATP) supplemented with 200 µM ATP for 45 min at 30°C. The reaction was stopped by addition of SDS denaturing buffer (Novex, ThermoFisher Scientific), followed by boiling for 5 min. The samples were then separated by SDS-PAGE, transferred onto PVDF membranes and probed with an antiphospho-c-Jun Ab (Cell Signaling Technology No. Cat No. 9164).

Statistical analysis. One-way analysis of variance was used to assess statistically significant differences between several groups. The Student Newman-Keul's test was then utilized for multiple comparisons. Kruskal-Wallis test was used with Dunn's multiple comparison for non-Normally distributed data. The software used for statistical analysis is SPSS Statistics for windows, V21.0, IBM (Corp, Armonk, New York). $P < .05$ was considered as significant for all tests.

RESULTS

Delayed 4MP Treatment Protects Against APAP-induced Liver Injury

Because in mice the metabolism of APAP is almost completed within 1.5 h after treatment with a dose of 300 mg/kg APAP (McGill *et al.*, 2013), we investigated the effect of delayed 4MP (50 mg/kg) administration in this model. APAP caused a time-dependent increase of plasma ALT activities (Figure 1A), development of centrilobular necrosis (Figs. 1B and 1D), and nuclear DNA strand breaks as indicated by the TUNEL assay at 6 h (Figure 1F). 4MP treatment 1.5 h after APAP effectively reduced all parameters of cell injury (Figs. 1A, 1C, 1E and 1G) suggesting that delayed 4MP treatment protects against APAP hepatotoxicity by an alternate mechanism than inhibition of CYP enzymes. However, the protection was lost when 4MP was administered 3 h after APAP (Supplemental Figure 1).

Delayed 4MP Treatment Protects by Inhibition of JNK

APAP toxicity depends on the amplification of the mitochondrial oxidant stress by activation of JNK in the cytosol and the translocation of phospho-JNK to the mitochondria (Hanawa *et al.*, 2008; Saito *et al.*, 2010a). JNK is present in the cytosol in the inactivated form and APAP treatment induced JNK activation in the cytosol at 3 and 6 h (Figs. 2A and 2B). In addition, P-JNK also translocated to the mitochondria at these time points (Figs. 2A and 2B). 4MP treatment at 1.5 h after APAP had no effect on cytosolic JNK activation at 3 h but eliminated the mitochondrial translocation (Figure 2A). At 6 h, 4MP prevented both cytosolic JNK activation and mitochondrial P-JNK translocation (Figure 2B). Because 4MP is treated at 1.5 h, ie, at a time where in the murine model JNK is already activated in the cytosol but P-JNK has not yet translocated to the mitochondria (Xie *et al.*, 2015), 4MP did not prevent JNK activation at 3 h. However, these data indicate that 4MP inhibits the sustained APAP-induced JNK activation and translocation to the mitochondria.

Delayed 4MP Treatment Does Not Block APAP Protein Adduct Formation

To further confirm that the delayed treatment with 4MP had no effect on the metabolic activation of APAP, protein adducts were measured at 3 and 6 h after APAP. There was no significant difference of APAP protein adducts between groups at 3 h (Figure 3A) suggesting that indeed 4MP had no effect on CYP-mediated reactive metabolite formation. However, the decline of adducts at 6 h was more pronounced in the 4MP-treated animals (Figure 3A). Removal of adducts is known to be caused by autophagy (Ni *et al.*, 2016). Thus, LC3 levels as indicator of autophagosome formation were assessed (Supplemental Figure 2A). 4MP treatment clearly caused an increase in LC3II levels compared to APAP alone at 3 h indicating that there is likely stimulated autophagy that could enhance the removal of adducts (Supplemental Figure 2A). Animals were treated with leupeptin, which inhibits lysosomal proteases and consequently autophagy (Ni *et al.*, 2016). Delayed 4MP treatment dramatically attenuated APAP-induced liver injury but leupeptin partially reversed this effect (Supplemental Figure 2B). Although the effect of leupeptin on plasma ALT activities was significant, the ALT levels were reduced from 97% with 4MP alone to 94% with 4MP + leupeptin indicating that the overall impact of lysosomal adduct removal on the protective effect of 4MP was minor.

Delayed Treatment of 4MP Blocks APAP-induced Mitochondrial Dysfunction

Amplification of the initial mitochondrial oxidant stress by JNK results in the collapse of the mitochondrial membrane potential leading to mitochondrial permeability transition pore (MPTP) opening (Kon *et al.*, 2004; Ramachandran *et al.*, 2011). This is followed by mitochondrial swelling and rupture of the mitochondrial outer membrane which then triggers the release of mitochondrial intermembrane protein including AIF to the cytosol and the nucleus (Bajt *et al.*, 2006, 2011). Consistent with the previous findings, although there was no AIF present in the cytosol of untreated mice, AIF release was observed at 6 h after APAP overdose (Figure 3B). 4MP treatment almost completely prevented any AIF release (Figure 3B) suggesting that 4MP prevented mitochondrial dysfunction.

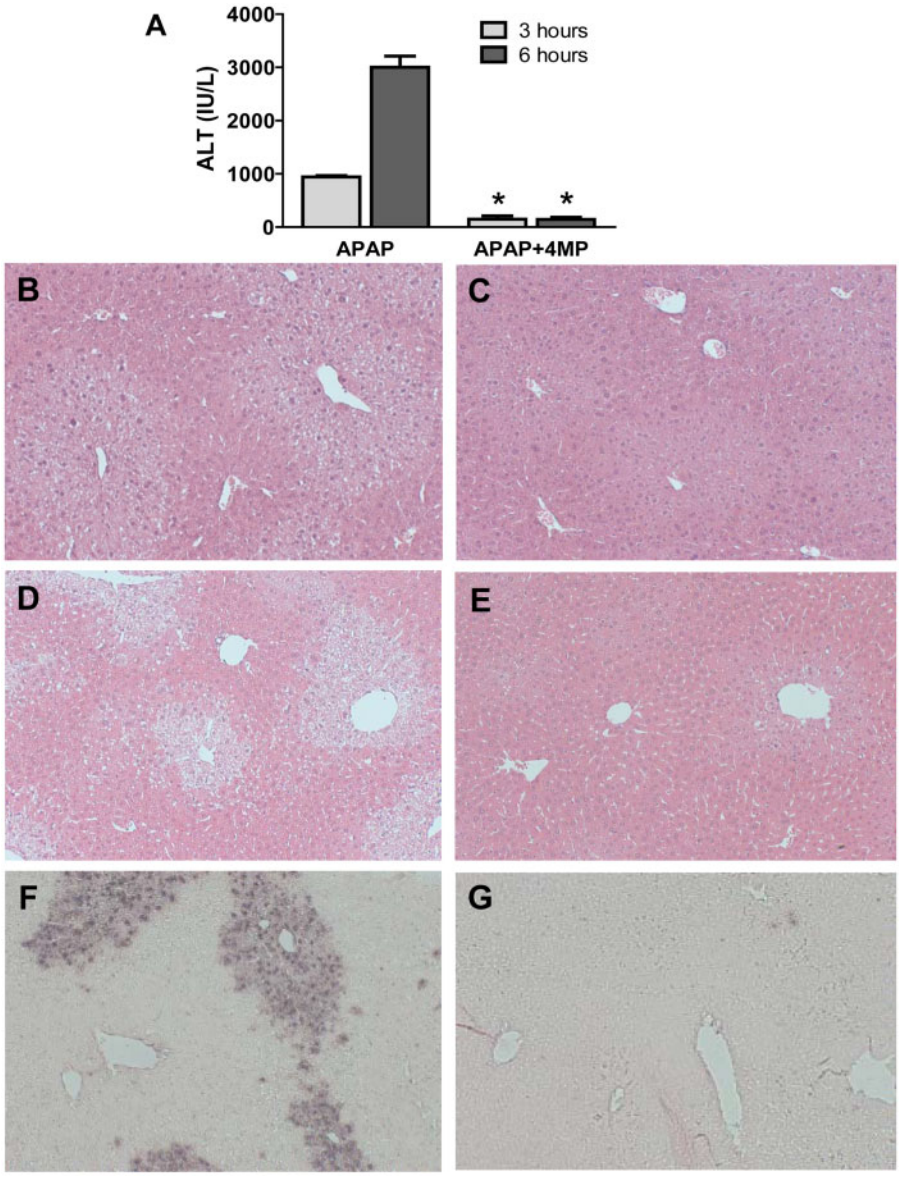

Figure 1. Delayed 4-methylpyrazole (4MP) treatment protects against acetaminophen (APAP)-induced liver injury. Animals were treated with 300 mg/kg APAP followed by 50 mg/kg 4MP 90 min after APAP. A, Plasma alanine aminotransferase (ALT) at 3 and 6 h after APAP. B, Representative hematoxylin and eosin (H&E)-stained liver section 3 h post-APAP. C, Three hours post-APAP and 4MP. D, Six hours post-APAP. E, Six hours post-APAP and 4MP (×50 magnification). F, Terminal deoxynucleotidyl transferase dUTP nick end labeling (TUNEL) staining (×50 magnification) shown for animals treated with APAP for 6 h and (G) for animals treated with APAP and 4MP for 6 h. Data represent means ± SEM of $n = 11$ animals per group. $^{*}p < .05$ (compared with animals treated with APAP alone).

After an APAP overdose, NAPQI depletes hepatic GSH levels by > 90% within 30 min and for a dose of 300 mg/kg, the recovery of the hepatic GSH content starts between 1.5 and 2 h (McGill *et al.*, 2013). Thus, the higher hepatic GSH levels in the 4MP-treated animals at 6 h compared to APAP alone reflects a better recovery due to a higher number of healthy cells (Figure 3C). In addition, the GSSG-to-GSH ratio, which is an indicator of mitochondrial oxidant stress (Jaeschke, 1990), shows substantially lower values in the 4MP-treated animals (Figure 3C). In fact, the values for the GSSG-to-GSH ratio of < 1% in the 4MP treated mice are close to control values (Knight *et al.*, 2001). These data indicate that 4MP treatment effectively prevented the APAP-induced mitochondrial oxidant stress and further supports the conclusion that 4MP inhibits mitochondrial dysfunction.

Because delayed inhibition of JNK could have detrimental effects on liver regeneration, this aspect was investigated. Animals were treated with APAP and then with solvent or 4MP 3 h later. At 24 h, the livers showed similar injury and PCNA staining suggesting that 4MP has no effect on hepatic regeneration (data not shown).

4MP Inhibits JNK Activation in Other Experimental Models

To evaluate if 4MP can inhibit JNK activation in models independent of APAP toxicity, we first used a model of JNK activation based on GSH depletion with phorone and t-butylhydroperoxide (tBHP)-induced oxidant stress (Saito *et al.*, 2010a). Three hours after phorone/tBHP treatment, extensive JNK activation was observed in the liver cytosol (Figure 4A) but no mitochondrial translocation (data not shown). 4MP treatment 1 h after tBHP

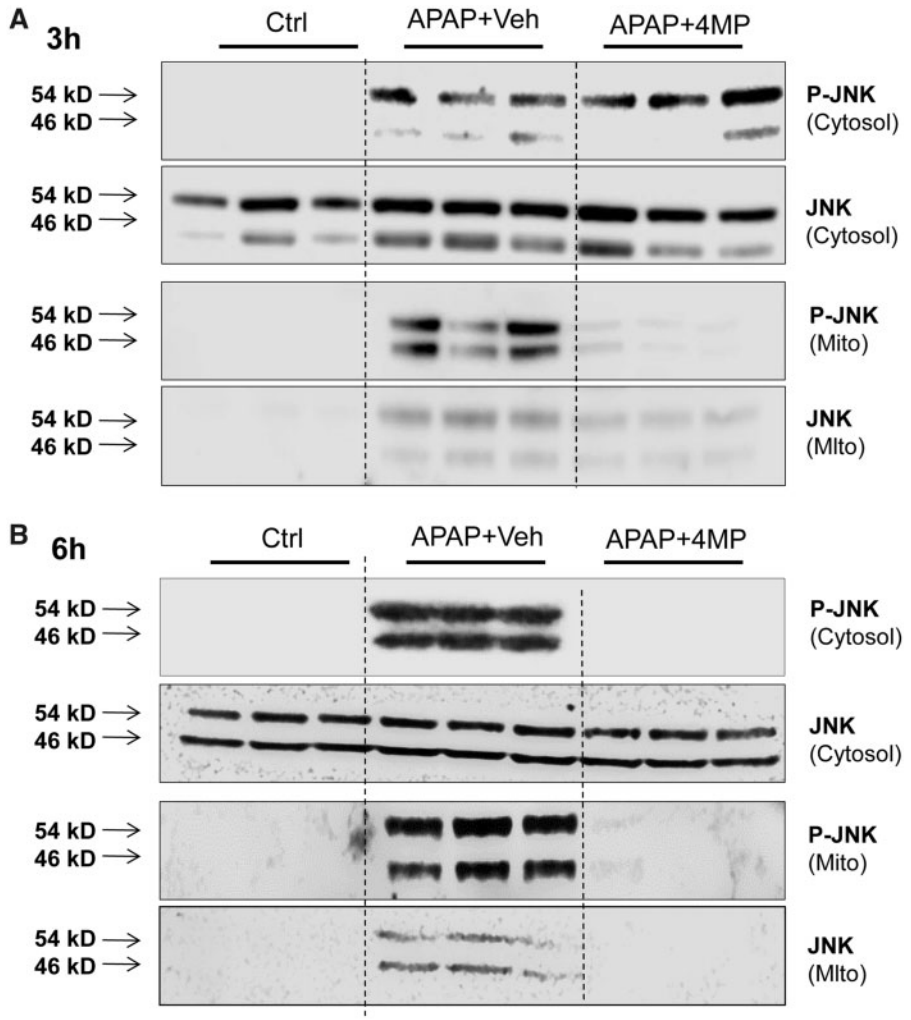

Figure 2. Delayed 4-methylpyrazole (4MP) treatment prevented acetaminophen (APAP)-induced sustained c-Jun n-terminal kinase (JNK) activation. Animals were treated with 300 mg/kg APAP followed by 50 mg/kg 4MP 90 min after APAP. Cytosolic fraction and isolated mitochondrial fraction were subjected to western blotting for P-JNK and JNK after 3 (A) and 6 h (B) after APAP. Three animals were analyzed per group.

effectively prevented JNK activation in the cytosol (Figure 4A). The Gal/ET model is a well-established model of apoptosis and inflammatory liver injury (Maes *et al.*, 2016), which also involves JNK activation (Wang *et al.*, 2006). Consistent with these previous findings, Gal/ET-induced liver injury as indicated by the elevated plasma ALT activities at 6 h (Figure 4B) and cytosolic JNK activation at 1 h, which is sustained until 6 h (Figure 4C). Cotreatment of 4MP with Gal/ET significantly attenuated liver injury and JNK activation in this model (Figs. 4B and 4C). Importantly, 4MP did not affect hepatic gene expression of TNF-α (Figure 4D), the critical cytokine in this model. Together, these data further support the conclusion that 4MP is a JNK inhibitor.

4MP Directly Docks into the Active Site of JNK1 and JNK2

To further analyze the putative binding of 4MP to JNK1 and JNK2, the molecular docking program AutoDock Vina was used to assess potential binding sites, poses, and energies of 4MP (Trott and Olson, 2010). We docked 4MP into both JNK1 and JNK2 as outlined in the methods; briefly, we deleted any previously published ligands from the structure, and then used a search box large enough to envelop the entire molecule to determine the binding mode and thermodynamics. To determine if the previously published structures of JNK1 and JNK2 were appropriate models for molecular docking, we attempted to reproduce the experimental binding modes for quercetagetin and BIRB796 to JNK1 and JNK2, respectively (PDB codes 3V3V and 3NPC) (Baek *et al.*, 2013; Kuglstatter *et al.*, 2010). Each ligand in the control docking experiments was bound in the same conformation as the previous structure's binding sites and poses (Figs. 5D–G). Therefore, our docking parameters were validated for JNK1 and JNK2. For the JNK1 and JNK2 molecular docking, both were observed to have thermodynamically favorable binding modes for 4MP into the ATP binding pocket of each enzyme, implying that the presence of 4MP may interfere with ATP binding (Figs. 5A and 5B). Additionally, we used a structure of Cyp2e1 bound to 4MP (PDB code 3E4E) to test 4MP's free energy of binding in a known structure (Porubsky *et al.*, 2008). Importantly, because the structure of 4MP bound to Cyp2e1 is known, molecular docking of 4MP into Cyp2e1 allows us to calculate the binding thermodynamics of 4MP in a known binding site, which we can then compare with our binding energies from JNK1 and JNK2. We found that both the binding site and orientation agreed well with the published structure (with RMSD of 1.86 Å between the experimental and computational binding modes), and that the free energy of binding was −4.2 kcal/mol (Figure 5C). This binding mode was calculated to

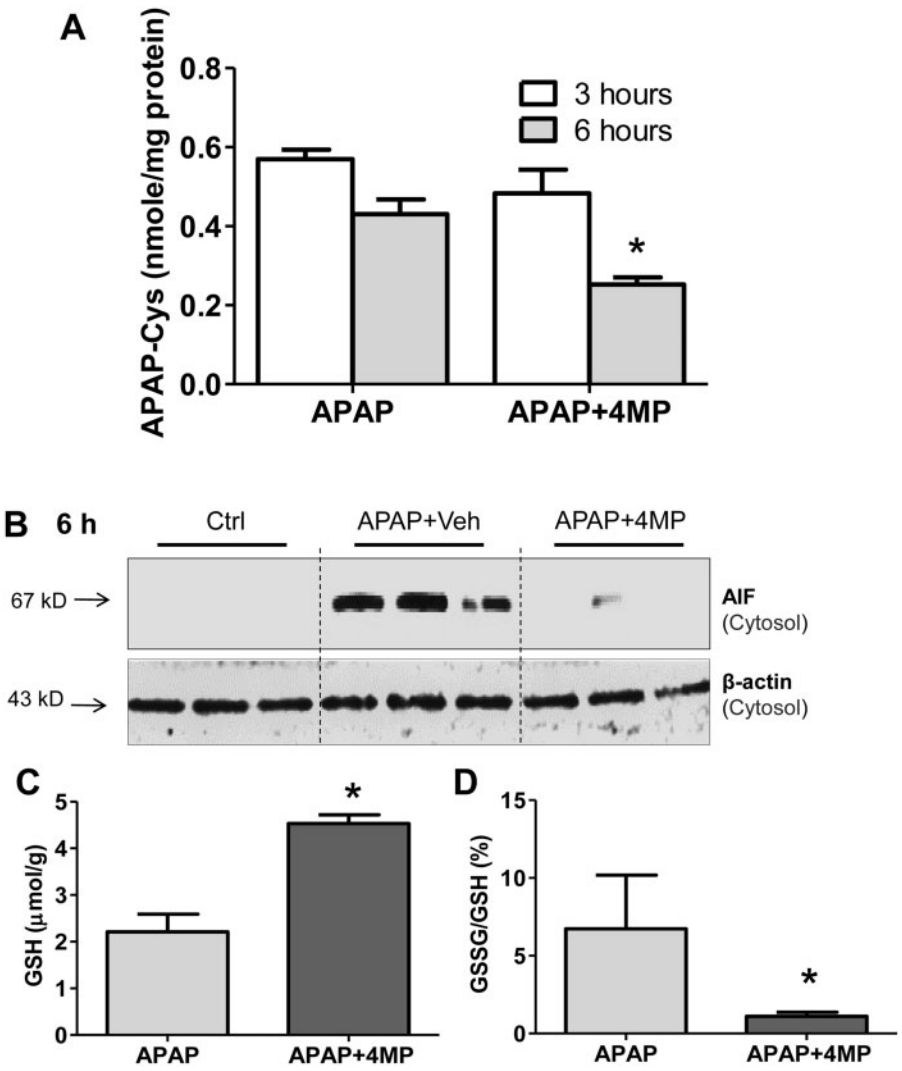

Figure 3. Delayed 4-methylpyrazole (4MP) treatment prevented acetaminophen (APAP)-induced mitochondrial dysfunction independent of reactive metabolite formation. Animals were treated with 300 mg/kg APAP followed by 50 mg/kg 4MP 90 min after APAP. A, APAP-cysteine adducts were quantified by HPLC-ECD in liver homogenate 3 and 6 h post-APAP treatment. B, Cytosolic fractions were subjected to western blotting for apoptosis-inducing factor (AIF) and β-actin. C, Total glutathione (GSH) was measured in liver tissue homogenate at 6 h post-APAP. D, The ratio of glutathione disulfide (GSSG) to total GSH was calculated. Data represent means ± SEM of $n = 6$ animals per group. *$p < .05$ (compared with animals treated with APAP alone).

be slightly more thermodynamically favorable than that of the binding energy of 4MP to JNK1 and JNK2 (at −3.3 and −3.5 kcal/mol, respectively) suggesting a lower binding affinity for JNK1 and JNK2 than for Cyp2e1. This implies that the dissociation constant for 4MP binding to JNK1 and JNK2 would be slightly higher than 2 µM, which is the published affinity for 4MP to Cyp2e1 (Collom *et al.*, 2008).

To demonstrate that 4MP is involved in target engagement with JNK, a thermal shift assay was carried out *in vitro* (Ishii *et al.*, 2017). As shown in Figure 5H, gradual JNK denaturation was evident in controls when exposed to increasing temperatures and exposure to 4MP decreased stability of JNK, making it susceptible to thermal denaturation at lower temperatures when compared to control. The aggregation temperature curve demonstrates the substantial negative shift induced by 4MP on the thermal stability of JNK. This suggests that 4MP binds to and destabilizes JNK. Thermal denaturation of 4MP treated samples was similar to those of samples treated with the JNK inhibitor SP600125 (data not shown).

To directly evaluate if 4MP interfered with JNK kinase activity, an *in vitro* kinase assay was carried out using activated phospho-JNK immunoprecipitated from liver samples of mice treated with Gal-ET for 1 h. As seen in Figure 5I, the presence of 4MP significantly inhibited phosphorylation of recombinant c-Jun when incubated with phospho-JNK and ATP. This also seems to be relevant *in vivo*, because our preliminary data indicate that administration of 4MP significantly decreases nuclear phospho-c-Jun staining by 3 h in liver sections from animals treated with phorone/tBHP (data not shown).

The JNK inhibitor SP600125 has been shown to also inhibit upstream kinases such as MKK4 (Bennett *et al.*, 2001) and our preliminary data suggest that animals treated with 4MP also show decreased MKK4 phosphorylation at 3 h (data not shown). However, this could be due to a block in amplification of mitochondrial oxidant stress due to JNK inhibition by 4MP. The lack of a direct inhibition of MKK4 by 4MP is also indicated by docking studies which suggest that interaction of 4MP with MKK4 occurs at a site independent of the ATP binding site (data not shown).

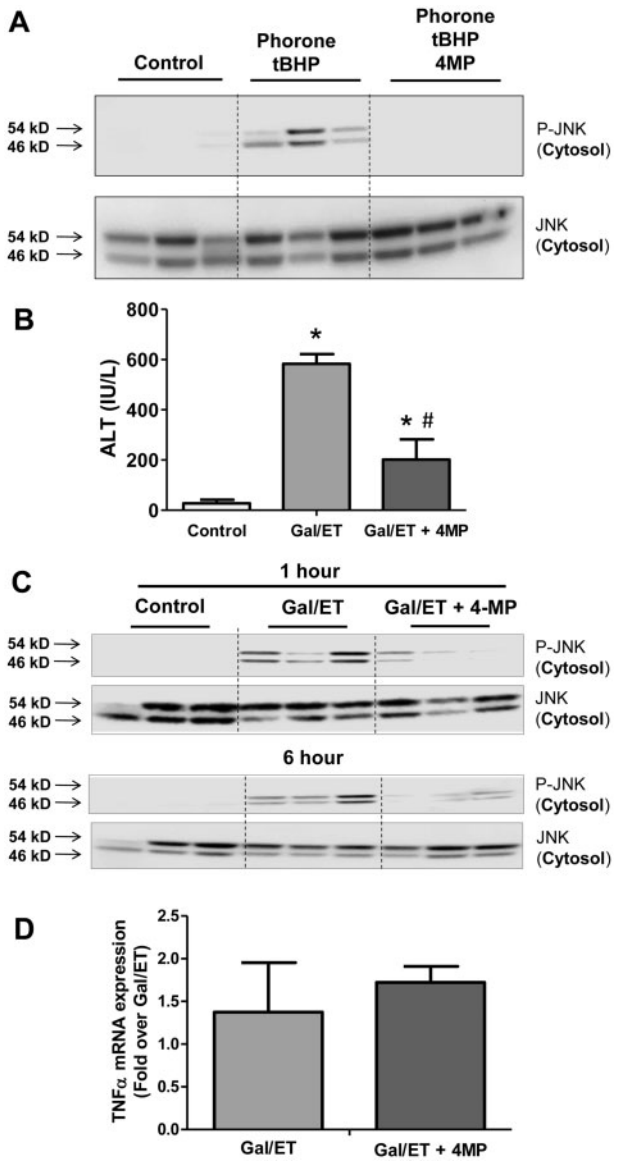

Figure 4. 4-Methylpyrazole (4MP) inhibits c-Jun n-terminal kinase (JNK) activation induced by glutathione (GSH) depletion and oxidant stress and injury and JNK activation in the D-galactosamine/endotoxin (Gal/ET) model. A, C57BL/6J mice were treated with 100 mg/kg phorone followed by 1 mmol/kg tBHP 1 h after phorone and 50 mg/kg 4MP 1 h after tBHP. At 6 h after tBHP cytosolic fractions were subjected to western blotting for P-JNK and JNK. For the Gal/ET model, C57BL/6J mice were cotreated with 700 mg/kg galactosamine, 100 μg/kg endotoxin, and 50 mg/kg 4MP for 1 and 6 h. B, Plasma alanine aminotransferase (ALT) at 6 h after Gal/ET. C, Cytosolic fractions were subjected to western blotting for P-JNK and JNK at 1 and 6 h after Gal/ET. D, TNF-α mRNA expression in liver samples at 1 h after Gal/ET. Data represent means ± SEM of $n = 6$ animals per group. *$p < .05$ (compared with control). #$p < .05$ (compared with Gal/ET).

Is 4MP More Effective Than NAC?

NAC is the only clinically approved antidote against APAP overdose. To compare the efficacy of both agents, animals were treated with either 50 mg/kg 4MP, 500 mg/kg NAC or both 90 min after APAP. Plasma ALT activities measurements at 6 and 24 h showed the extensive injury after APAP and the high efficacy of both compounds alone and in combination (Figure 6A). There was a trend of slightly higher injury after 4MP treatment compared to NAC and the combination at 24 h. Using a higher dose of 4MP (200 mg/kg) did not affect the results, suggesting that the generally used 50 mg/kg dose was most effective (Figure 6A). When the dose of APAP was increased to 600 mg/kg, both NAC and 4MP reduced APAP-induced liver injury by >90% (Figure 6B). However, 4MP was slightly more effective than NAC at these doses (Figure 6B).

DISCUSSION

Protection With Delayed 4MP Treatment

Our previous study showed that cotreatment of 4MP with an APAP overdose effectively eliminated hepatotoxicity by inhibiting the CYP-dependent metabolic activation of APAP in mice and in human hepatocytes (Akakpo *et al.*, 2018). The objective of the current investigation was to evaluate if a delayed treatment with 4MP beyond the metabolism phase is still protective. The metabolism of the commonly used overdose of 300 mg/kg in C57BL/6J mice takes approximately 90 min (McGill *et al.*, 2013). Thus, when using a delayed treatment, 50 mg/kg 4MP was still highly effective in protecting against APAP hepatotoxicity at 6 and 24 h. Interestingly, the protection was lost when the treatment was pushed back to 3 h. In addition, a higher dose of 4MP was not more effective. These data suggest that the therapeutic window for the beneficial effects of 4MP after an APAP overdose extends beyond the drug metabolism phase.

4MP Acts as JNK Inhibitor

The delayed treatment with 4MP showed a marked inhibition of JNK activation at 6 h and mitochondrial P-JNK translocation at 3 and 6 h after APAP in mice. JNK is activated in the cytosol within 1 h after APAP and P-JNK can translocate to the mitochondria after 2 h (Xie *et al.*, 2015). Thus, 4MP given after 90 min was administered after the initial activation but before the mitochondrial translocation explaining why the early JNK activation was not prevented. However, JNK activation at 6 h was inhibited, which supports the previously proposed hypothesis that continuous JNK activation and mitochondrial translocation are necessary to aggravate the oxidant stress and induce the MPTP opening with necrotic cell death (Hu *et al.*, 2016). Further support for the effect of 4MP on JNK activation was the attenuated oxidant stress and the reduced release of the intermembrane protein AIF, which is in part responsible for the nuclear DNA fragmentation as indicated by the TUNEL assay (Bajt *et al.*, 2011). Together, these data are consistent with the hypothesis that the main mechanism of protection of the delayed 4MP treatment involves inhibition of JNK activation.

To provide further support for this mechanism of action of 4MP, additional models of hepatic JNK activation were used. One model mimics the events of APAP overdose where its initial mitochondrial oxidant stress under conditions of GSH depletion can activate the redox-sensitive apoptosis signal-regulating kinase 1, a member of the mitogen-activated protein kinase kinase kinase family, which eventually leads to JNK activation (Nakagawa *et al.*, 2008; Xie *et al.*, 2015). Treatment of animals with phorone to deplete hepatic GSH followed by the injection of a peroxide induces JNK activation (Saito *et al.*, 2010a). 4MP effectively prevented this JNK activation consistent with its effect as a JNK inhibitor. The second, well-established model of JNK activation is Gal/ET-induced apoptosis and inflammatory liver injury (Maes *et al.*, 2016). TNF-α is thought to be the critical mediator of the pathophysiology in part through the prolonged activation of JNK (Wang *et al.*, 2006). Like what was previously shown, Gal/ET-induced JNK activation at 1 and 6 h and liver injury at 6 h. 4MP strongly attenuated both JNK activation and

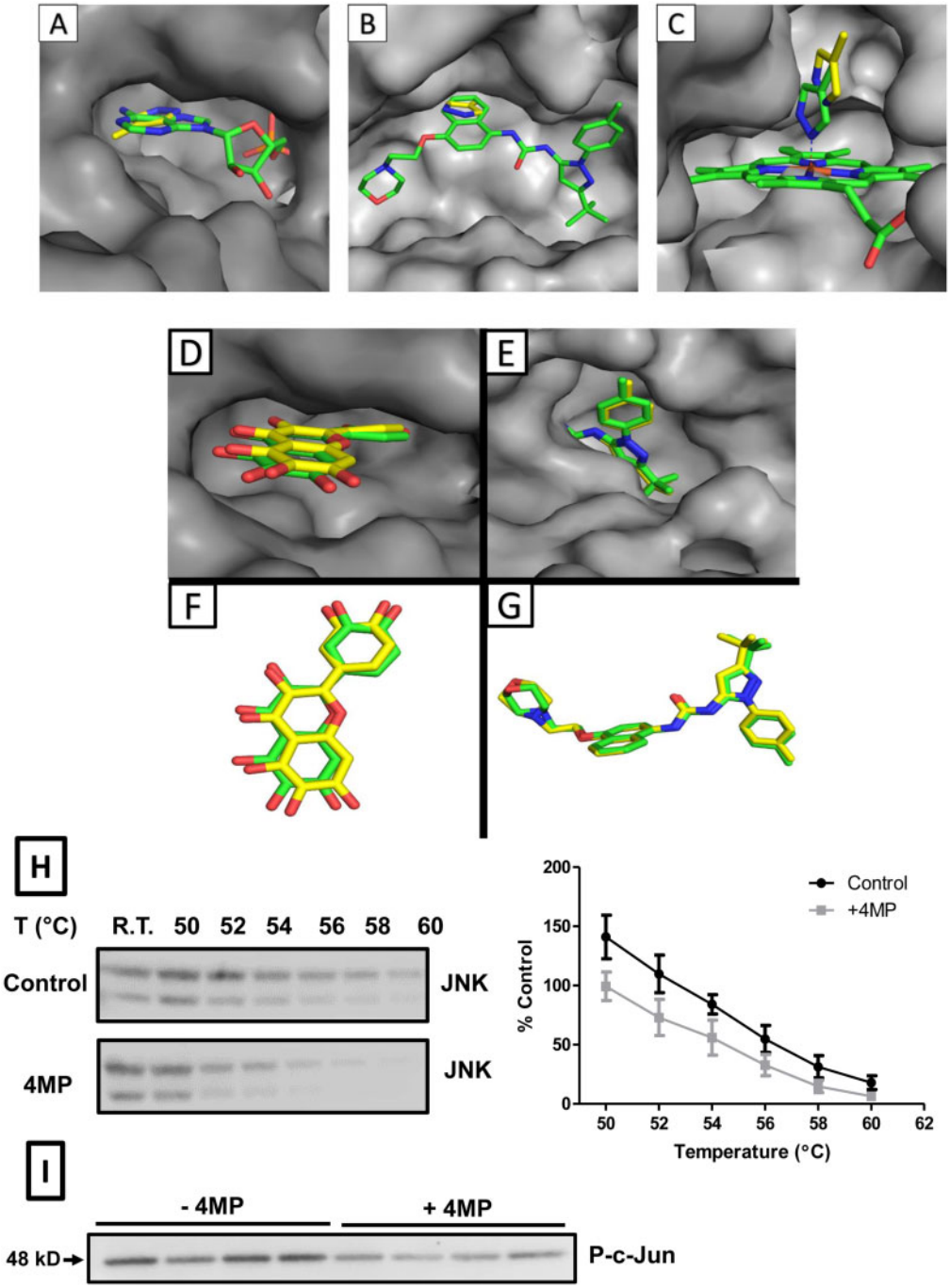

Figure 5. 4-Methylpyrazole (4MP) docks into the active site and destabilize both c-Jun n-terminal kinase (JNK)1 and JNK2. Snapshots of 4MP molecular docking results. A, Binding site and pose of docked 4MP (yellow sticks) compared with previously published structure of JNK1 (gray surface) bound to an ATP analog (green/dark gray sticks). B, 4MP (yellow/light gray sticks) docked into the ATP binding site of JNK2 (gray surface), overlaid with a structure of the inhibitor BIRB796 (green/dark gray sticks), a compound demonstrated to prevent ATP binding. C, Binding site and orientation of docked 4MP (yellow/light gray sticks) compared to the published structure of Cyp2e1 (gray surface) with 4MP and the heme moiety (green/dark gray sticks). Each structure has portions of the enzyme removed for clarity, and PDB codes 3E4E, 3V3V, 3NPC were used. Control docking experiments. D and E, Overlays from 2 angles of a published structure of quercetagetin (green/dark gray sticks) bound to JNK1 (gray surface) with the docked binding mode (yellow/light gray sticks). F and G, Two views of a structure of JNK2 (gray surface) bound to BIRB796 (green sticks) superimposed with the docked binding mode of BIRB796 (yellow/light gray sticks). H, Detection of soluble protein in the supernatant fraction by Western blot and aggregation temperature curve from cellular thermal shift assay (CETSA) assay to evaluate 4MP-JNK binding *in vitro*. I, Hepatic JNK enzyme activity was assayed *in vitro* in the presence or absence of 2 mM 4MP using a c-Jun recombinant protein as the substrate.

liver injury. Importantly, 4MP did not affect TNF-α gene expression. Again, this is consistent with an effect of 4MP on JNK activation. Together, these data in 2 *in vivo* models independent of APAP toxicity also suggest that 4MP acts as JNK inhibitor. This effect of 4MP on JNK activity seems to be rather unique, because other CYP inhibitors such as piperonyl butoxide, which have been shown to protect against APAP overdose (Brady *et al.*, 1988), are unlikely to inhibit JNK activity (Kawai *et al.*, 2009).

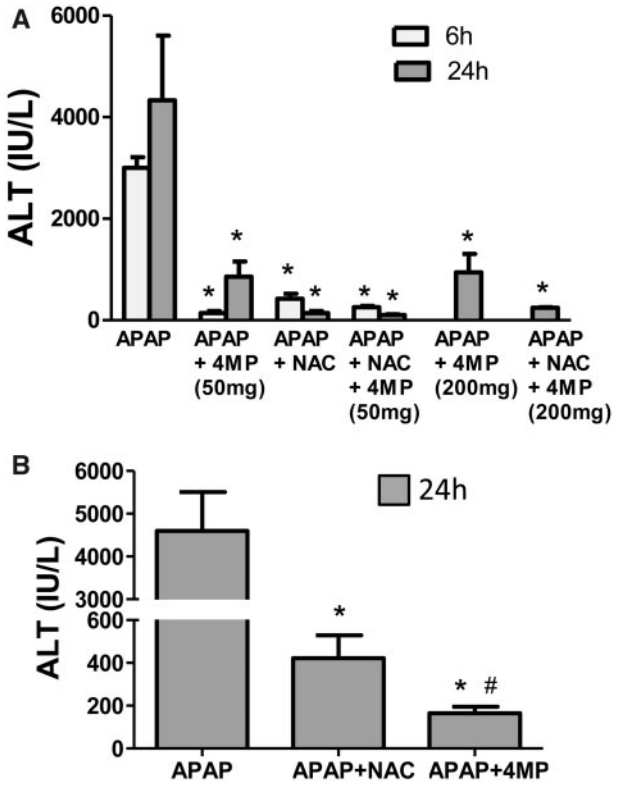

Figure 6. Efficacy of 4-methylpyrazole (4MP) versus N-acetylcysteine (NAC). C57BL/6J mice were treated with 300 mg/kg acetaminophen (APAP) for 6 and 24 h followed by 50 mg/kg 4MP, 200 mg/kg 4MP, or 500 mg/kg NAC alone or in combination 90 min after APAP. A, Plasma alanine aminotransferase (ALT) of 6 and 24 h post-APAP. B, Animals were treated with 600 mg/kg APAP followed by 50 mg/kg 4MP 90 min later. Plasma ALT 24 h post-APAP. Data represent means ± SEM of $n = 9$ animals per group. *$p < .05$ (compared with APAP alone). #$p < .05$ (compared with APAP + NAC).

To investigate the interaction between 4MP and JNK, the molecular docking program AutoDock Vina was used to analyze potential binding sites and the binding energies of 4MP for both JNK1 and JNK2 and the results compared to Cyp2e1 (Trott and Olson, 2010), which is known to be inhibited by 4MP. The data clearly demonstrated that both JNK1 and JNK2 have thermodynamically favorable binding modes for 4MP into the ATP binding pocket of each enzyme, implying that the presence of 4MP may interfere with ATP binding. This would render its inhibition like that of SP600125, a hydrophobic ATP-competitive JNK inhibitor (Heo *et al.*, 2004). The binding energies of 4MP to JNK1 and JNK2 were only slightly less thermodynamically favorable than the calculated binding energy of 4MP to Cyp2e1. These data are consistent with 4MP being an effective inhibitor of both JNK1 and JNK2. The *in silico* binding studies are corroborated by the *in vitro* thermal shift assay, which clearly indicates that exposure to 4MP decreases thermal stability of JNK. With thermal shift assays, both increases and decreases in thermal stability suggest binding; studies with elacridar, a representative inhibitor of the multidrug-resistance transporter MDR1, showed that the drug elicited a destabilizing effect on its target, probably due to a loss of ATP and its stabilizing effect on the transporter (Reinhard *et al.*, 2015). Thus, 4MP may elicit a transient destabilizing effect on JNK by binding at the active site where the ATP phosphate group binds. This is turn would block productive ATP binding and hydrolysis leading to the loss of ATP and its stabilizing effect on JNK.

Effect of 4MP on Autophagy

Autophagy is a critical adaptation process to cellular stress to remove modified proteins and cell organelles (Chao *et al.*, 2018). The cellular debris is packaged into autophagosomes, which fuse with lysosomes for degradation of its content. In APAP hepatotoxicity, removal of mitochondria (Ni *et al.*, 2012) and protein adducts (Ni *et al.*, 2016) by autophagy has been shown to limit the extent of liver injury. Our current data suggest that 4MP accelerates the clearance of APAP protein adducts by inducing autophagy. This process can be blocked with the lysosomal inhibitor leupeptin (Ni *et al.*, 2016). Because leupeptin had only a very limited impact on the protective effect of 4MP, the contribution of lysosomal protein adduct removal to 4MP's overall mechanism of protection appears very limited.

How Does the Efficacy of 4MP as Antidote Against APAP Hepatotoxicity Compare With NAC?

A critical question remains how the protective effect of 4MP compares to NAC. The protective mechanisms of 4MP include the inhibition of Cyp enzymes (Akakpo *et al.*, 2018) and JNK. On the other hand, NAC stimulates hepatic GSH synthesis, which then can scavenge NAPQI (Corcoran *et al.*, 1985) and later peroxynitrite and reactive oxygen (Saito *et al.*, 2010b); in addition, a surplus of NAC can be converted to Krebs cycle intermediates, which support the impaired mitochondrial bioenergetics (Saito *et al.*, 2010b). Thus, both compounds are effective antidotes against APAP hepatotoxicity, however, with different but complementary mechanisms. A direct comparison of 4MP and NAC alone and in combination using the 300 mg/kg APAP dose and 90 min post-treatment showed similarly effective protection in mice. There was only a very minor difference in ALT activities with NAC being more protective. However, when the same treatment of NAC and 4MP was used with a higher dose of APAP (600 mg/kg), 4MP was significantly more effective than NAC. Because it takes substantially longer than 90 min to metabolize this dose of APAP in mice (McGill *et al.*, 2013), both protective mechanisms are operative for each compound, ie, inhibition of Cyps and JNK for 4MP and scavenging of NAPQI and ROS for NAC. These data suggest that 4MP may be more effective in cases of severe overdoses with prolonged metabolism. These mechanisms of protection of 4MP may be particularly relevant for patients for several reasons: First, in contrast to experimental studies where APAP is dissolved in saline, patients who intentionally overdose generally take tablets and use even higher overdoses than employed in the mouse model, which leads to prolonged absorption and metabolism. Second, the activation of JNK and its mitochondrial translocation is more delayed in human hepatocytes (6–15 h after APAP) (Xie *et al.*, 2014) compared to mice (1–2 h) (Xie *et al.*, 2015) leading to a more delayed peak of injury after an APAP overdose in patients (48–72 h) (Larson, 2007; McGill *et al.*, 2012a) compared to mice (12–24 h) (McGill *et al.*, 2013). This explains why in the mouse almost all interventions beyond 2.5 h are no longer effective (James *et al.*, 2003; Knight *et al.*, 2002). In humans, this process is substantially delayed, which may make 4MP similar to NAC effective much longer than in mice. Third, to prevent toxicity it appears more advantageous to prevent NAPQI formation (4MP) than to scavenge it (NAC) and to prevent JNK activation and the aggravation of the mitochondrial oxidant stress (4MP) rather than to scavenge ROS (NAC). Thus, based on the complementary therapeutic targets affecting the same mechanisms, which are operative both in mice and in humans, we can conclude that 4MP is as effective as antidote against APAP hepatotoxicity as the standard of care intervention NAC. However, an advantage of 4MP over

NAC is that it acts directly and does not require additional metabolism as NAC, which needs to be converted to GSH. Thus, under special circumstances, eg, a patient with a defect in enzymes required for GSH synthesis, 4MP may be more effective. In addition, in patients who develop an anaphylactic reaction to NAC treatment, which affects more than 10% of patients (Yamamoto *et al.*, 2014), 4MP may be a better alternative. Lastly, patients who take a very high overdose, a combination of 4MP and NAC may be more effective than NAC alone. However, these assumptions are based on the mechanistic insight in the mouse model and would need to be verified in patients. Nevertheless, our mechanistic data provide a strong rationale for evaluating 4MP in patients.

CONCLUSIONS

Our data indicate that treatment with 4MP beyond the metabolism phase of APAP is still highly protective in the murine model. The main mechanism of protection is that 4MP can effectively inhibit JNK activation and thus prevent the aggravation of the mitochondrial oxidant stress and mitochondrial dysfunction. The inhibition of JNK by 4MP was further confirmed in 2 additional experimental models. Moreover, docking studies support the hypothesis that 4MP can reversibly bind to the ATP binding site of JNK. Thus, 4MP is an effective antidote against APAP hepatotoxicity with protective mechanisms complementary to NAC.

SUPPLEMENTARY DATA

Supplementary data are available at *Toxicological Sciences* online.

FUNDING

This work was supported by a grant from McNeil Consumer Health Care, Inc, the National Institutes of Health grants (R01 DK102142, to HJ and R35 GM128562 to BF), and the National Institute of General Medical Sciences (P20 GM103549 and P30 GM118247 to HJ) from the National Institutes of Health. J.Y.A. was supported by an NIH Predoctoral Fellowship (F31 DK120194-01).

DECLARATION OF CONFLICTING INTERESTS

The authors declared no potential conflicts of interest with respect to the research, authorship, and/or publication of this article.

REFERENCES

Adams, P. D., Afonine, P. V., Bunkoczi, G., Chen, V. B., Davis, I. W., Echols, N., Headd, J. J., Hung, L. W., Kapral, G. J., Grosse-Kunstleve, R. W., *et al.* (2010). PHENIX: A comprehensive Python-based system for macromolecular structure solution. *Acta Crystallogr. D. Biol. Crystallogr.* **66**, 213–221.

Akakpo, J. Y., Ramachandran, A., Kandel, S. E., Ni, H. M., Kumer, S. C., Rumack, B. H., and Jaeschke, H. (2018). 4-Methylpyrazole protects against acetaminophen hepatotoxicity in mice and in primary human hepatocytes. *Hum. Exp. Toxicol.* **37**, 1310–1322.

Baek, S., Kang, N. J., Popowicz, G. M., Arciniega, M., Jung, S. K., Byun, S., Song, N. R., Heo, Y. S., Kim, B. Y., Lee, H. J., *et al.* (2013). Structural and functional analysis of the natural JNK1 inhibitor quercetagetin. *J. Mol. Biol.* **425**, 411–423.

Bajt, M. L., Cover, C., Lemasters, J. J., and Jaeschke, H. (2006). Nuclear translocation of endonuclease G and apoptosis-inducing factor during acetaminophen-induced liver cell injury. *Toxicol. Sci.* **94**, 217–225.

Bajt, M. L., Ramachandran, A., Yan, H. M., Lebofsky, M., Farhood, A., Lemasters, J. J., and Jaeschke, H. (2011). Apoptosis-inducing factor modulates mitochondrial oxidant stress in acetaminophen hepatotoxicity. *Toxicol. Sci.* **122**, 598–605.

Barceloux, D. G., Krenzelok, E. P., Olson, K., and Watson, W. (1999). American academy of clinical toxicology practice guidelines on the treatment of ethylene glycol poisoning. Ad hoc committee. *J. Toxicol. Clin. Toxicol.* **37**, 537–560.

Bekka, R., Borron, S. W., Astier, A., Sandouk, P., Bismuth, C., and Baud, F. J. (2001). Treatment of methanol and isopropanol poisoning with intravenous fomepizole. *J. Toxicol. Clin. Toxicol.* **39**, 59–67.

Bennett, B. L., Sasaki, D. T., Murray, B. W., O'Leary, E. C., Sakata, S. T., Xu, W., Leisten, J. C., Motiwala, A., Pierce, S., Satoh, Y., *et al.* (2001). SP600125, an anthrapyrazolone inhibitor of Jun N-terminal kinase. *Proc. Natl. Acad. Sci. U.S.A.* **98**, 13681–13686.

Bestic, M., Blackford, M., and Reed, M. (2009). Fomepizole: A critical assessment of current dosing recommendations. *J. Clin. Pharmacol.* **49**, 130–137.

Brady, J. T., Montelius, D. A., Beierschmitt, W. P., Wyand, D. S., Khairallah, E. A., and Cohen, S. D. (1988). Effect of piperonyl butoxide post-treatment on acetaminophen hepatotoxicity. *Biochem. Pharmacol.* **37**, 2097–2099.

Brennan, R. J., Mankes, R. F., Lefevre, R., Raccio-Robak, N., Baevsky, R. H., DelVecchio, J. A., and Zink, B. J. (1994). 4-Methylpyrazole blocks acetaminophen hepatotoxicity in the rat. *Ann. Emerg. Med.* **23**, 487–494.

Brent, J., McMartin, K., Phillips, S., Aaron, C., and Kulig, K. (2001). Methylpyrazole for toxic alcohols study G. Fomepizole for the treatment of methanol poisoning. *N. Engl. J. Med.* **344**, 424–429.

Budnitz, D. S., Lovegrove, M. C., and Crosby, A. E. (2011). Emergency department visits for overdoses of acetaminophen-containing products. *Am. J. Prev. Med.* **40**, 585–592.

Chao, X., Wang, H., Jaeschke, H., and Ding, W. X. (2018). Role and mechanisms of autophagy in acetaminophen-induced liver injury. *Liver Int.* **38**, 1363–1374.

Collom, S. L., Laddusaw, R. M., Burch, A. M., Kuzmic, P., Perry, M. D., Jr., and Miller, G. P. (2008). CYP2E1 substrate inhibition. Mechanistic interpretation through an effector site for monocyclic compounds. *J. Biol. Chem.* **283**, 3487–3496.

Corcoran, G. B., Racz, W. J., Smith, C. V., and Mitchell, J. R. (1985). Effects of N-acetylcysteine on acetaminophen covalent binding and hepatic necrosis in mice. *J. Pharmacol. Exp. Ther.* **232**, 864–872.

Corcoran, G. B., and Wong, B. K. (1986). Role of glutathione in prevention of acetaminophen-induced hepatotoxicity by N-acetyl-L-cysteine in vivo: studies with N-acetyl-D-cysteine in mice. *J. Pharmacol. Exp. Ther.* **238**, 54–61.

Dai, Y., and Cederbaum, A. I. (1995). Cytotoxicity of acetaminophen in human cytochrome P4502E1-transfected HepG2 cells. *J. Pharmacol. Exp. Ther.* **273**, 1497–1505.

Gujral, J. S., Knight, T. R., Farhood, A., Bajt, M. L., and Jaeschke, H. (2002). Mode of cell death after acetaminophen overdose in mice: Apoptosis or oncotic necrosis? *Toxicol. Sci.* **67**, 322–328.

Hanawa, N., Shinohara, M., Saberi, B., Gaarde, W. A., Han, D., and Kaplowitz, N. (2008). Role of JNK translocation to mitochondria leading to inhibition of mitochondria bioenergetics in acetaminophen-induced liver injury. *J. Biol. Chem.* **283**, 13565–13577.

Hazai, E., Vereczkey, L., and Monostory, K. (2002). Reduction of toxic metabolite formation of acetaminophen. *Biochem. Biophys. Res. Commun.* **291**, 1089–1094.

Heo, Y. S., Kim, S. K., Seo, C. I., Kim, Y. K., Sung, B. J., Lee, H. S., Lee, J. I., Park, S. Y., Kim, J. H., Hwang, K. Y., *et al.* (2004). Structural basis for the selective inhibition of JNK1 by the scaffolding protein JIP1 and SP600125. *Embo. J.* **23**, 2185–2195.

Hu, J., Ramshesh, V. K., McGill, M. R., Jaeschke, H., and Lemasters, J. J. (2016). Low dose acetaminophen induces reversible mitochondrial dysfunction associated with transient c-Jun N-terminal kinase activation in mouse liver. *Toxicol. Sci.* **150**, 204–215.

Ishii, T., Okai, T., Iwatani-Yoshihara, M., Mochizuki, M., Unno, S., Kuno, M., Yoshikawa, M., Shibata, S., Nakakariya, M., Yogo, T., *et al.* (2017). CETSA quantitatively verifies in vivo target engagement of novel RIPK1 inhibitors in various biospecimens. *Sci. Rep.* **7**, 13000.

Jaeschke, H. (1990). Glutathione disulfide formation and oxidant stress during acetaminophen-induced hepatotoxicity in mice in vivo: The protective effect of allopurinol. *J. Pharmacol. Exp. Ther.* **255**, 935–941.

Jaeschke, H., McGill, M. R., and Ramachandran, A. (2012). Oxidant stress, mitochondria, and cell death mechanisms in drug-induced liver injury: Lessons learned from acetaminophen hepatotoxicity. *Drug Metab. Rev.* **44**, 88–106.

James, L. P., McCullough, S. S., Lamps, L. W., and Hinson, J. A. (2003). Effect of N-acetylcysteine on acetaminophen toxicity in mice: Relationship to reactive nitrogen and cytokine formation. *Toxicol. Sci.* **75**, 458–467.

Kawai, M., Saegusa, Y., Jin, M., Dewa, Y., Nishimura, J., Harada, T., Shibutani, M., and Mitsumori, K. (2009). Mechanistic study on hepatocarcinogenesis of piperonyl butoxide in mice. *Toxicol. Pathol.* **37**, 761–769.

Knight, T. R., Ho, Y. S., Farhood, A., and Jaeschke, H. (2002). Peroxynitrite is a critical mediator of acetaminophen hepatotoxicity in murine livers: protection by glutathione. *J. Pharmacol. Exp. Ther.* **303**, 468–475.

Knight, T. R., Kurtz, A., Bajt, M. L., Hinson, J. A., and Jaeschke, H. (2001). Vascular and hepatocellular peroxynitrite formation during acetaminophen toxicity: Role of mitochondrial oxidant stress. *Toxicol. Sci.* **62**, 212–220.

Kon, K., Kim, J. S., Jaeschke, H., and Lemasters, J. J. (2004). Mitochondrial permeability transition in acetaminophen-induced necrosis and apoptosis of cultured mouse hepatocytes. *Hepatology* **40**, 1170–1179.

Kucukardali, Y., Cinan, U., Acar, H. V., Ozkan, S., Top, C., Nalbant, S., Cermik, H., Cankir, Z., and Danaci, M. (2002). Comparison of the therapeutic efficacy of 4-methylpyrazole and N-acetylcysteine on acetaminophen (paracetamol) hepatotoxicity in rats. *Curr. Med. Res. Opin.* **18**, 78–81.

Kuglstatter, A., Ghate, M., Tsing, S., Villasenor, A. G., Shaw, D., Barnett, J. W., and Browner, M. F. (2010). X-ray crystal structure of JNK2 complexed with the p38alpha inhibitor BIRB796: Insights into the rational design of DFG-out binding MAP kinase inhibitors. *Bioorg. Med. Chem. Lett.* **20**, 5217–5220.

Larson, A. M. (2007). Acetaminophen hepatotoxicity. *Clin. Liver Dis.* **11**, 525–548.

Maes, M., Vinken, M., and Jaeschke, H. (2016). Experimental models of hepatotoxicity related to acute liver failure. *Toxicol. Appl. Pharmacol.* **290**, 86–97.

Manthripragada, A. D., Zhou, E. H., Budnitz, D. S., Lovegrove, M. C., and Willy, M. E. (2011). Characterization of acetaminophen overdose-related emergency department visits and hospitalizations in the United States. *Pharmacoepidemiol. Drug Saf.* **20**, 819–826.

Mateus, A., Maatta, T. A., and Savitski, M. M. (2016). Thermal proteome profiling: Unbiased assessment of protein state through heat-induced stability changes. *Proteome Sci.* **15**, 13.

McGill, M. R., and Jaeschke, H. (2015). A direct comparison of methods used to measure oxidized glutathione in biological samples: 2-Vinylpyridine and N-ethylmaleimide. *Toxicol. Mech. Methods* **25**, 589–595.

McGill, M. R., Lebofsky, M., Norris, H. R., Slawson, M. H., Bajt, M. L., Xie, Y., Williams, C. D., Wilkins, D. G., Rollins, D. E., and Jaeschke, H. (2013). Plasma and liver acetaminophen-protein adduct levels in mice after acetaminophen treatment: Dose-response, mechanisms, and clinical implications. *Toxicol. Appl. Pharmacol.* **269**, 240–249.

McGill, M. R., Sharpe, M. R., Williams, C. D., Taha, M., Curry, S. C., and Jaeschke, H. (2012a). The mechanism underlying acetaminophen-induced hepatotoxicity in humans and mice involves mitochondrial damage and nuclear DNA fragmentation. *J. Clin. Invest.* **122**, 1574–1583.

McGill, M. R., Williams, C. D., Xie, Y., Ramachandran, A., and Jaeschke, H. (2012b). Acetaminophen-induced liver injury in rats and mice: Comparison of protein adducts, mitochondrial dysfunction, and oxidative stress in the mechanism of toxicity. *Toxicol. Appl. Pharmacol.* **264**, 387–394.

Mitchell, J. R., Jollow, D. J., Potter, W. Z., Gillette, J. R., and Brodie, B. B. (1973). Acetaminophen-induced hepatic necrosis. IV. Protective role of glutathione. *J. Pharmacol. Exp. Ther.* **187**, 211–217.

Morris, G. M., Huey, R., Lindstrom, W., Sanner, M. F., Belew, R. K., Goodsell, D. S., and Olson, A. J. (2009). AutoDock4 and AutoDockTools4: Automated docking with selective receptor flexibility. *J. Comput. Chem.* **30**, 2785–2791.

Nakagawa, H., Maeda, S., Hikiba, Y., Ohmae, T., Shibata, W., Yanai, A., Sakamoto, K., Ogura, K., Noguchi, T., Karin, M., *et al.* (2008). Deletion of apoptosis signal-regulating kinase 1 attenuates acetaminophen-induced liver injury by inhibiting c-Jun N-terminal kinase activation. *Gastroenterology* **135**, 1311–1321.

Nelson, S. D. (1990). Molecular mechanisms of the hepatotoxicity caused by acetaminophen. *Semin. Liver Dis.* **10**, 267–278.

Ni, H. M., Bockus, A., Boggess, N., Jaeschke, H., and Ding, W. X. (2012). Activation of autophagy protects against acetaminophen-induced hepatotoxicity. *Hepatology* **55**, 222–232.

Ni, H. M., McGill, M. R., Chao, X., Du, K., Williams, J. A., Xie, Y., Jaeschke, H., and Ding, W. X. (2016). Removal of acetaminophen protein adducts by autophagy protects against acetaminophen-induced liver injury in mice. *J. Hepatol.* **65**, 354–362.

Porubsky, P. R., Meneely, K. M., and Scott, E. E. (2008). Structures of human cytochrome P-450 2E1. Insights into the binding of inhibitors and both small molecular weight and fatty acid substrates. *J. Biol. Chem.* **283**, 33698–33707.

Ramachandran, A., and Jaeschke, H. (2018). Acetaminophen toxicity: Novel Insights Into Mechanisms and Future Perspectives. *Gene Expr.* **18**, 19–30.

Ramachandran, A., Lebofsky, M., Baines, C. P., Lemasters, J. J., and Jaeschke, H. (2011). Cyclophilin D deficiency protects against acetaminophen-induced oxidant stress and liver injury. *Free Radic. Res.* **45**, 156–164.

Reinhard, F. B., Eberhard, D., Werner, T., Franken, H., Childs, D., Doce, C., Savitski, M. F., Huber, W., Bantscheff, M., Savitski, M. M., *et al.* (2015). Thermal proteome profiling monitors ligand interactions with cellular membrane proteins. *Nat. Methods* **12**, 1129–1131.

Rumack, B. H., and Bateman, D. N. (2012). Acetaminophen and acetylcysteine dose and duration: Past, present and future. *Clin. Toxicol. (Phila)* **50**, 91–98.

Saito, C., Lemasters, J. J., and Jaeschke, H. (2010a). c-Jun N-terminal kinase modulates oxidant stress and peroxynitrite formation independent of inducible nitric oxide synthase in acetaminophen hepatotoxicity. *Toxicol. Appl. Pharmacol.* **246**, 8–17.

Saito, C., Zwingmann, C., and Jaeschke, H. (2010b). Novel mechanisms of protection against acetaminophen hepatotoxicity in mice by glutathione and N-acetylcysteine. *Hepatology* **51**, 246–254.

Smilkstein, M. J., Knapp, G. L., Kulig, K. W., and Rumack, B. H. (1988). Efficacy of oral N-acetylcysteine in the treatment of acetaminophen overdose. Analysis of the national multicenter study (1976 to 1985). *N. Engl. J. Med.* **319**, 1557–1562.

Trott, O., and Olson, A. J. (2010). AutoDock Vina: Improving the speed and accuracy of docking with a new scoring function, efficient optimization, and multithreading. *J. Comput. Chem.* **31**, 455–461

Wang, Y., Singh, R., Lefkowitch, J. H., Rigoli, R. M., and Czaja, M. J. (2006). Tumor necrosis factor-induced toxic liver injury results from JNK2-dependent activation of caspase-8 and the mitochondrial death pathway. *J. Biol. Chem.* **281**, 15258–15267.

Xie, Y., McGill, M. R., Dorko, K., Kumer, S. C., Schmitt, T. M., Forster, J., and Jaeschke, H. (2014). Mechanisms of acetaminophen-induced cell death in primary human hepatocytes. *Toxicol. Appl. Pharmacol.* **279**, 266–274.

Xie, Y., Ramachandran, A., Breckenridge, D. G., Liles, J. T., Lebofsky, M., Farhood, A., and Jaeschke, H. (2015). Inhibitor of apoptosis signal-regulating kinase 1 protects against acetaminophen-induced liver injury. *Toxicol. Appl. Pharmacol.* **286**, 1–9.

Yamamoto, T., Spencer, T., Dargan, P. I., and Wood, D. M. (2014). Incidence and management of N-acetylcysteine-related anaphylactoid reactions during the management of acute paracetamol overdose. *Eur. J. Emerg. Med.* **21**, 57–60.

Yip, L., and Heard, K. (2016). Potential adjunct treatment for high-risk acetaminophen overdose. *Clin. Toxicol. (Phila)* **54**, 459.

Yoon, E., Babar, A., Choudhary, M., Kutner, M., and Pyrsopoulos, N. (2016). Acetaminophen-induced hepatotoxicity: A comprehensive update. *J. Clin. Transl. Hepatol.* **4**, 131–142.

Zell-Kanter, M., Coleman, P., Whiteley, P. M., and Leikin, J. B. (2013). A gargantuan acetaminophen level in an acidemic patient treated solely with intravenous N-acetylcysteine. *Am. J. Ther.* **20**, 104–106.